

Full Length Article

Blue phosphorene nanosheets with point defects: Electronic structure and hydrogen storage capability

Daughty John ^{a,b}, Bijoy Nharangatt ^a, Srihari Madhav Kastuar ^a, Raghu Chatanathodi ^{a,*}^a Department of Physics, National Institute of Technology Calicut, Calicut, Kerala 673601, India^b Department of Physics, Mohammed Abdurahiman Memorial Orphanage College, Calicut, Kerala 673601, India

ARTICLE INFO

Keywords:

Two dimensional materials
Point defects
Adsorption
Hydrogen storage
DFT

ABSTRACT

Presence of defects in two dimensional nanomaterial can lead to dramatic changes in their structural and electronic properties. Through *ab-initio* DFT computations, we study the electronic structure of semiconducting 2D elemental monolayers of blue phosphorene, with common point defects like Stone-Wales, single and double vacancies. The calculated formation energies of single and double vacancies in phosphorene are found to be lower compared to other well known 2D monolayers. Electronic structure of blue phosphorene shows a reduced band gap from that of the perfect lattice, and flat bands characterizing the defect states. We also investigate the suitability of defective blue phosphorene as a hydrogen storage template. We find that, like in the case of perfect phosphorene nanosheets, metal decoration of defective phosphorene can enhance the storage capacity for hydrogen molecules, with binding energies suitable for practical storage. Lithium decoration of the single and double vacancy defect at higher coverage can store a maximum of six to nine hydrogen molecules per defect, thus leading to a high gravimetric density of hydrogen. It is found that these structures are stable at room temperature. Comparing the storage capabilities of defective black and blue phosphorene, we find that defective blue phosphorene can store more hydrogen than black phosphorene.

1. Introduction

Two-dimensional materials, like graphene, silicene etc., possess fascinating structural and electronic properties, leading to wide ranging applications in electronic and opto-electronic devices [1–5]. Phosphorene [6] is the elemental phosphorus monolayer, stable in two allotropic forms, namely black and blue phosphorene. Black phosphorene monolayer is obtained from bulk through mechanical exfoliation [7], and is a buckled structure, unlike graphene. Buckled or non-planar structures are very common in the world of 2D materials, with silicene [5], borophene [8–10] and 2D transition metal di-chalcogenides like MoS₂ [11] showing prominent departure from planar geometry. Blue phosphorene (blue-P) is different from black phosphorene (black-P), having a zig-zag structure sideways, while the black-P has an armchair structure. One can obtain the blue-P structure from the black-P structure through specific dislocations [12]. The blue-P allotrope was predicted computationally by Zhu et al. [12] and recently synthesized by Zhang et al. through an epitaxial growth method [13]. The band gaps for both allotropes are different, with 1.5 eV for black-P [14] and 2 eV for blue-P [12]. The band gap is thickness dependent and is lower in the bulk. In case of black-P,

the gap is direct, while blue-P it is indirect. Weak van der Waals (vdW) interaction between layers makes exfoliation easy in these materials. The relative stability of black compared to blue is found to be greater in case of free standing samples, while this is reversed in case samples deposited over various substrates [15].

Defects are universally present in real materials, with 2D materials being no exceptions. Defects that have been vigorously studied over the last few years in graphene [16], hexagonal boron nitride [17] and silicene [19] include Stone-Wales (SW), single vacancy (SV), double vacancy (DV) defects and ad-atoms. These are local point defects, which are a result of processing of 2D materials for applications in devices or sensors, through exposure to high energy radiation, electrons, ions etc. It is known that graphene gets magnetized with SV defect and also when C ad-atom is adsorbed [18], while silicene shows a magnetic moment only when an Si ad-atom is adsorbed and not in any of the other defects [19]. In both graphene and silicene, SW and DV type of defects remain non-magnetic, but introduce a small gap in the electronic band structure. Even though the formation energy of defects in graphene is very high (above 4 eV for Stone-Wales and above 6 eV for single and double vacancy), we still have experimental proofs of their existence [16]. Defects

* Corresponding author.

E-mail address: raghuc@nitc.ac.in (R. Chatanathodi).

in the lattice may therefore provide opportunities to tailor properties like band-gap, reactivity and thermal stability of the 2D material, and are therefore worth exploring.

Fig. 1 displays some of the point defects found in blue-P. Since blue-P is structurally similar to silicene, we have considered the same defects for blue-P as found in case of silicene. The Stone-Wales defect is created by rotating a P-P bond in the 2D lattice by 90° about the center of the bond (**Fig. 1(a)**) which results in the formation of two pentagons and two heptagons in the place of four hexagons and is denoted as SW-(55|77). Since the only operation involved is rotation, the number of atoms in the system remains the same and there will be no dangling bonds. **Fig. 1(b)** depicts an SV-(5|9) in blue-P (which is termed SV-2 in silicene), obtained by deleting a single P atom, leading to the formation of a pentagon and a 9-edged chain of atoms. **Fig. 1(c)** represents a DV-(5|8|5), so designated due to the formation of two pentagons and a chain of 8P atoms, caused due to removal of two P-atoms. **Fig. 1(d)** is the DV-(555|777) defect which is also caused by removal of two P atoms. Specifically, graphene, silicene and black phosphorene show SW, SV-(5|9), DV-(5|8|5), DV-(555|777) defects. There exist several computational and experimental studies that explore the nature of these defects and the changes they cause in electronic structure and properties of graphene, silicene and black-P [16,19,20].

Elaborate computational studies of these defects in black-P have been already undertaken by Hu and Yang [12], where the structure permits ten kinds of distinct point defects, under the categories of SW, SV and DV. It is found that these defects in black-P form much more easily than in graphene or silicene and are thermally stable. Of these ten, it is found that only three can induce changes in electronic structure of black-P. To be specific, Hu and Yang report that the SV-(5|9) and DV-(5|8|5) bring changes to the fundamental band gap of black-P, the SV-(5|9) and SV-(55|66) defects lead to hole doping, and the SV-(5|9) can also result in net magnetic moment.

The unique buckled surface structure of both phosphorene allotropes opens up wide ranging prospects of using phosphorene as catalysts, sensors and templates for energy storage. Non-planar surface, combined with a strain dependent energy band gap makes black-P a suitable photo catalyst [21]. Studies have also shown phosphorene to be a good anode material for Li and Na ion storage batteries with high specific capacities [22,23]. The stability of adsorbed Li and Na ions on phosphorene have led to exploration of the possibility of hydrogen storage. Hydrogen is a

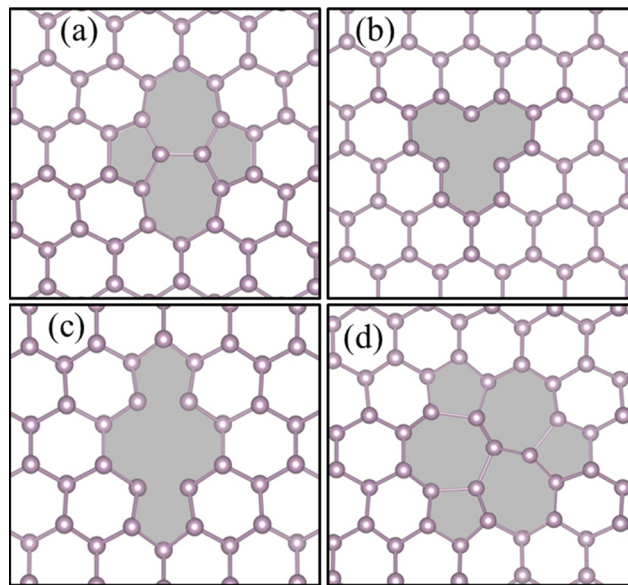


Fig. 1. Depiction of point defects in blue-P: (a) Stone-Wales (SW-(55|77)), (b) Single vacancy (SV-(5|9) or SV-2), (c) Double vacancy DV-(5|8|5) and (d) Double vacancy (DV-(555|777)).

clean and renewable source of energy, and one of the important alternatives to fossil fuels [24], which are diminishing fast while also being source of extensive environmental damage. To be of practical use as a fuel, it is convenient to store hydrogen in a form where it is adsorbed onto a substrate [25], but is easily released on a small stimulus. For this, H₂ adsorption energy should ideally be in the range of 0.1 eV – 1.0 eV [26,27]. Since 2D nanomaterials have a large surface area to volume ratio, they turn out to be very suitable templates to store H₂. Recent research work has yielded several 2D metal oxide, hydride and boride nanomaterials and clusters which show excellent capacity for storage of hydrogen, with and without metal decoration, motivating us to widely explore the existing world of 2D materials for new possibilities in H₂ storage [50–55]. In case of elemental 2D nanostructures, it is found that on defect free graphene, silicene or phosphorene, H₂ molecules adsorb with a binding energy that is too small to be of any practical use. It was then predicted, through a significant body of literature, that decorating nanomaterials like nanotubes, fullerenes and 2D nanostructures with light metal atoms would improve the capacity to hold H₂ molecules [28–35,29–36]. Yu et. al. computationally modeled H₂ adsorption on Li and Na decorated black-P [36], finding adsorption energies to be in the favorable range. They also found black-P yields a gravimetric ratio of 4.4% for stored H₂, upon increasing metal coverage. In a previous work, we have extended these studies to blue-P, confirming that H₂ can be stored on blue-P too, by Li or Na decoration, yielding a larger gravimetric ratio of 5.5% [37]. We find that in Li decorated blue-P, a maximum of four H₂ could be stored per unit cell, unlike the case Li decorated black-P, where only three H₂ could be stored. It is observed that a unit cell of black-P contains four P atoms and one adsorption site (hollow site), while a unit cell of blue-P has only two P atoms and one adsorption site (valley site). This is the main reason why the number of hydrogen molecules that can be adsorbed is higher in blue-P compared to black-P, which is computationally demonstrated in [37]. It may be expected that defective phosphorene, with metal decoration may support increased H₂ storage, due to the presence of unfulfilled bonds. In case of black-P, such a study has been undertaken recently, by Halder et al. [38] which concludes that the presence of point-defects in pristine black-P does not aid adsorption and storage. They do however find that Li decoration of the SV defect can yield good values for adsorption energy, and improve the gravimetric storage capacity to 5.3%.

In this paper, we systematically study the stability and electronic structure of the possible point defects in two dimensional blue-P. We describe and analyse how the Density of States (DOS) and band dispersion of defect free blue-P changes due to the presence of point defects. Beyond this, we investigate how H₂ molecules adsorb on defective blue-P. We then look at adsorption of a light metal like Li on the point defect sites on blue-P nanosheets, and how H₂ molecule binds to these metal atoms. The nature of binding is discussed through analysis of DOS and charge density. Ab-initio Molecular Dynamics (MD) is used to assess the stability of adsorbed molecules as temperature increases. Finally, we study how H₂ adsorption depends on coverage of adsorbed Li. In our study, we have not calculated the electronic structure of black-P, as several detailed studies have already done so, as mentioned above. However, we have computed characteristics of H₂ storage on both black and blue phosphorene, in order to compare and contrast the situation on both these substrates. In the remaining sections of this paper, we give details of the calculations undertaken, then state and discuss our main results and finally summarize and conclude.

2. Computational methodology

The calculations reported are carried out using the plane wave DFT method as implemented in the Vienna Ab initio Simulation Package (VASP) [39,40]. Projector Augmented Wave (PAW) potentials as characterized by Perdew, Burke, and Ernzerhof (PBE) [41] within the Generalized Gradient Approximation (GGA) are used. Van der Waals (vdW) interaction plays an important role in hydrogen adsorption in

phosphorene, as understood by our earlier studies [37]. vdW correction to total energy is included using the empirical DFT-D2 method of Grimme [42], which is less expensive computationally, compared to the superior non-local vdW density functionals (vdW-DF) [43], but without resulting in any significant loss of accuracy in results. The cut off for plane wave energy was fixed at 500 eV, and the system was relaxed using conjugate gradient method until the forces on each atom were below 0.01 eV/Å. A $4 \times 4 \times 1$ Monkhorst-Pack k-point grid [44] was used for sampling the reciprocal space. A vacuum slab of 20 Å was introduced in the z-direction to avoid interaction between the periodic systems. The basis set, k-point grid and vacuum layer dimensions used were tested rigorously for convergence. In order to obtain input defective structures for VASP calculations, the required defect was created in a structure optimized blue-P sheet, and the structure with the defect was again optimized. The formation energy of defects may be calculated from the equation, $E_f = E_{\text{defect}} - (N_p^* E_p)$; where E_{defect} is the total energy of the blue-P sheet with the defect, N_p is the number of P atoms in the defective blue-P and E_p energy per phosphorus atom in a perfect sheet. The supercell size required to contain the defects were fixed on basis of convergence of defect formation energies, up to 1 meV. The adsorption energy of several H₂ molecules on alkali decorated defective blue-P substrate is calculated using $E_{ad}^{(n)} = (E_{Li} - P^{(n-1)} + E_{H_2}) - E_{Li-P}^{(n)}$ where the superscript refers to the number of H₂ molecules already adsorbed on the substrate i.e., lithium decorated defective blue-P.

3. Results and discussion

3.1. Structure and energy of point defects

The geometry optimized structure obtained for blue-P nanosheet is shown in Fig. 2 with the unit cell marked. The converged values of the lattice constants of the hexagonal lattice are $a_1 = a_2 = 3.28\text{ \AA}$, the P-P bond length is 2.26 Å and the bond angle is 93°, which is very close to the values originally calculated by Zhu et al. [12]. The buckling height, of the structure is 1.24 Å. First, we investigate the geometry of the possible point defects. The optimized geometries of all the possible point defects in blue-P are shown in Fig. 3.

We find that in case of blue-P, the SV-(55|66) defect relaxes to SV-(5|9) defect, unlike in black-P or graphene and silicene. Hence, it not discussed further as a distinct entity in this paper. The SV-(5|9) defect has

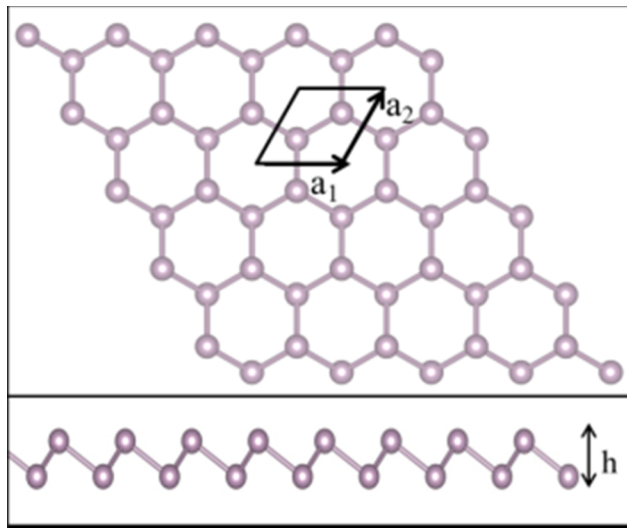


Fig. 2. The top (above) and side (below) views of the optimized structure of 5x5 supercell of blue-P. The lattice parameters are $a_1 = a_2 = 3.28\text{ \AA}$ and buckling height h is 1.24 Å.

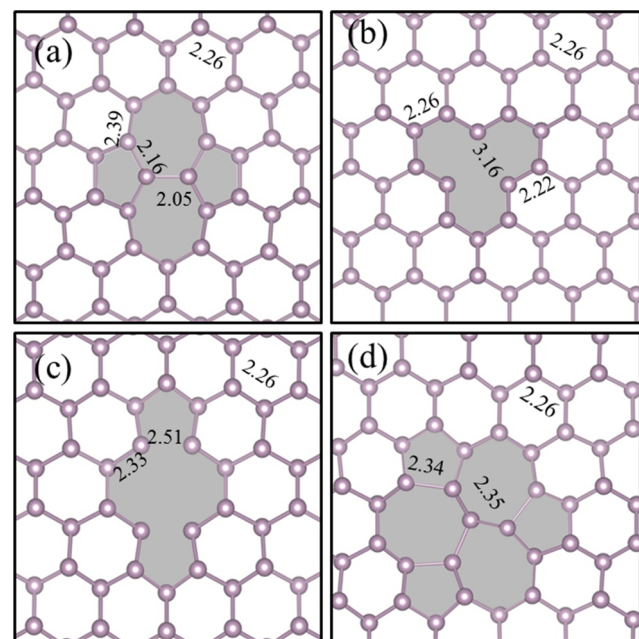


Fig. 3. The optimized structures of a) SW, b) SV-(5|9), c) DV-(5|8|5) and d) DV-(555|777) defects in blue-P.

three dangling bonds and is found to be less favored in silicene [19]. In DV-(5|8|5), the bonds are elongated up to 2.51 Å, while the original P-P bond length in the pristine blue-P is 2.26 Å. In DV-(555|777) defect, six hexagons restructure themselves into three pentagons and three heptagons. Here, the bonds in the vicinity of the defect undergo stretching by about 0.1 Å from the bond length in perfect blue-P. The formation energy, the magnetic moment and the band gap (calculated from band structure) of different defective phosphorene sheets is given in Table 1.

The SV-(5|9) defect has unpaired electrons due to dangling bonds, and hence a spin polarized calculation is performed. A magnetic moment 1.0 μ_B is obtained in SV-(5|9) defect, similar to the case of black-P [20]. It is observed that the energy required to form two single vacancy defects is far higher than the energy required for a double vacancy defect. So, the single vacancies will ultimately diffuse together to form double vacancy defects [19].

The formation energies of defects in blue-P are compared with those in graphene, silicene and black-P from literature in Table 2. From the values of formation energies, we can see that the SV-(55|66) defect is more probable over the SV-(5|9) defect in silicene, but in case of black-P it is the reverse. It can be seen that, as the buckling height increases from graphene (0.0 Å), through silicene (0.44 Å) to blue-phosphorene (1.24 Å), the formation energies show a decrease, except for the Stone-Wales defect. That means, on irradiation with laser or electron beams, these defects will be formed much easily in blue-P compared to graphene or silicene. Comparing between the phosphorene allotropes, the values suggest that the defects are relatively easily formed in black-P than in blue-P.

Table 1

The formation energy, magnetic moment and band gap for all point defects in blue-P.

	$E_f(\text{eV})$	μ	$E_g(\text{eV})$
Pristine	0.0	0.0	1.98
SW	3.69	0.0	0.32
SV-(5 9)	2.48	1.03	0 (up); 0.76 (down)
DV-(5 8 5)	2.91	0.0	0.88
DV-(555 777)	2.65	0.0	1.37

Table 2

The formation energies of different point defects in graphene, silicene, black and blue phosphorene (in eV). The SV-(55|66) defect is not formed in graphene and blue-P at all.

	SW	SV-(55 66)	SV-(5 9)	DV-(5 8 5)	DV-(555 777)
Graphene [16]	4.5	—	7.8	7.52	6.4
Silicene [19]	2.09	3.01	3.77	3.70	2.84
Black-P [20]	1.01–1.32	2.03	1.63	1.91–3.04	2.08–2.61
Blue-P	3.69	—	2.48	2.91	2.65

3.2. Electronic structure and charge density profile of defects

Calculated electronic structures of pristine and defective blue-P are displayed, as DOS in Fig. 4 and band dispersion in Fig. 5. The DOS and band structure (Figs. 4(a) and 5(a)) reaffirm the fact that blue-P is an indirect semi-conductor with a bad gap 1.8 eV [12].

The P atoms in blue-P may be considered to be a mix of sp^2 - sp^3 hybridized states (the bond angle is not 109.5°), and 3p_z orbital is populated with a lone pair of electrons. The valence and conduction bands are primarily made of 3p_z, 3p_x, 3p_y and 3s states. In the presence of defects, the band gap varies from 0.32 to 1.37 eV, remaining indirect in all cases, as seen in the band dispersions in Fig. 5(b)–(e). For the SW defect, there is a tiny gap of 0.32 eV (Fig. 4(b)) just above the Fermi level. This is also seen from the band dispersion in Fig. 5(b).

Fig. 4(c) shows that the SV-(5|9) defect makes blue-P into a magnetic semi-conductor, with one spin channel being metallic and the other

semiconducting, with a small gap of 0.76 eV. Due to the dangling bonds formed by the removal of a P atom bonded to three other P atoms in SV-(5|9), new defect states are formed. These states are close to the Fermi energy (Fig. 5(c)), seen as almost flat, dispersionless bands, implying localized nature of the defects. Here, the conduction band minimum is at the k-point M and the valence band maximum is at the k-point K, when the spin down is taken into consideration, showing that this is an indirect band gap. The new bands introduced in SV-(5|9) and DV-(5|8|5) can be looked upon as formed due to hole doping, since they are formed close to the valence band edge, while the new bands in SW defect, leading to a considerable lowering of the band gap can be looked upon as hole and electron doping. In DV-(555|777), there is no significant lowering of the band gap.

While there are only four distinct point defects in silicene and blue-P, there are ten point defects in black-P. This makes it difficult to compare the electronic structures of different defects of blue and black-P. In general, we can say that in all the defects which involve bond elongation or bond breaking, in both allotropes, new bands come into picture and they are of localized states in nature, as seen from their energy dispersion.

3.3. Adsorption of hydrogen molecules on defects

Next, we investigate the suitability of defective blue-P for H₂ adsorption and storage. First, we try to bind hydrogen molecules on to different sites on a defect. We find that the hollow site is the most favorable for adsorption, as shown in Fig. 6. Pristine blue-P sheet binds hydrogen molecules very weakly (binding energy is much less than 0.1

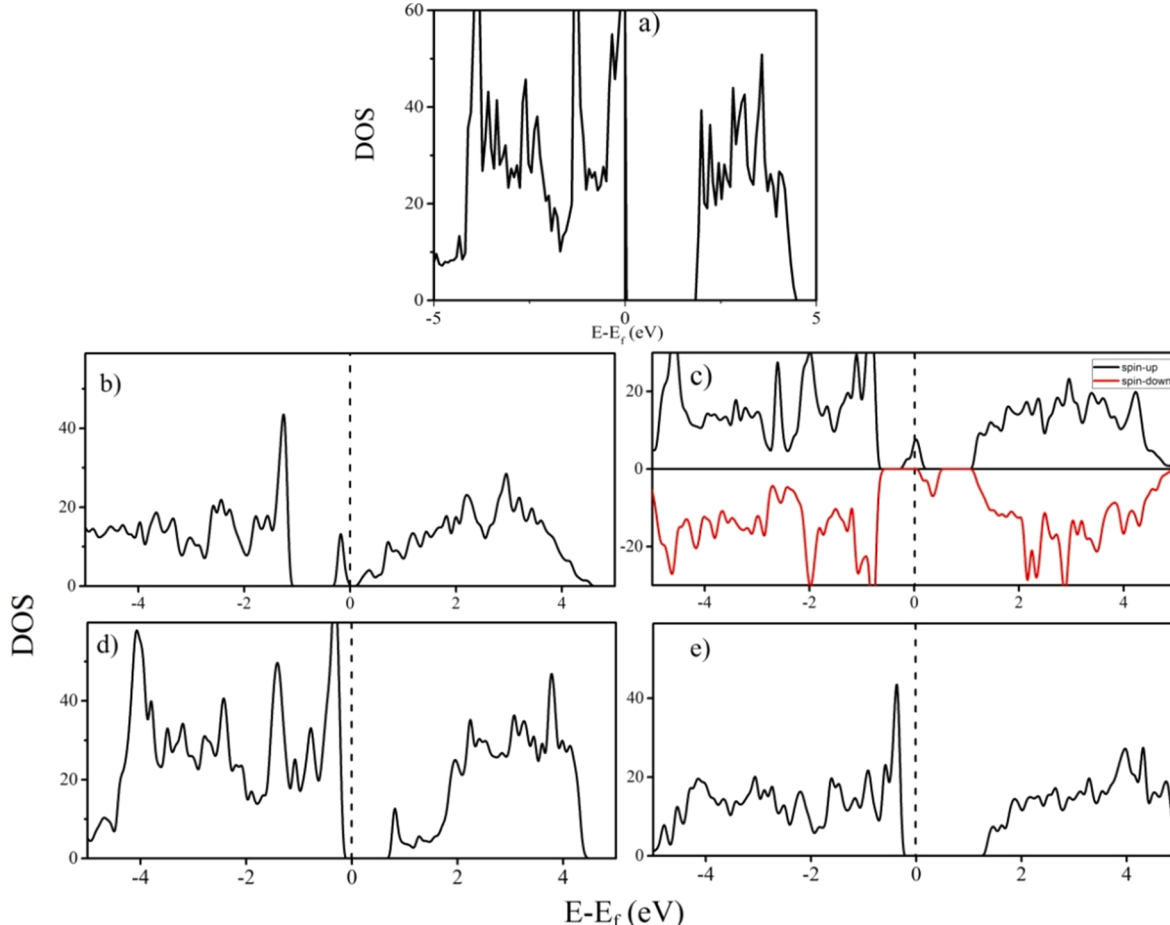


Fig. 4. The total DOS plots of (a) Pristine blue-P; (b) SW; (c) SV-(5|9); (d) DV-(5|8|5); and (e) DV-(555|777) defects in blue-P. The black line (red line) in (c) represents majority (minority), i.e. up (down) spin carriers.

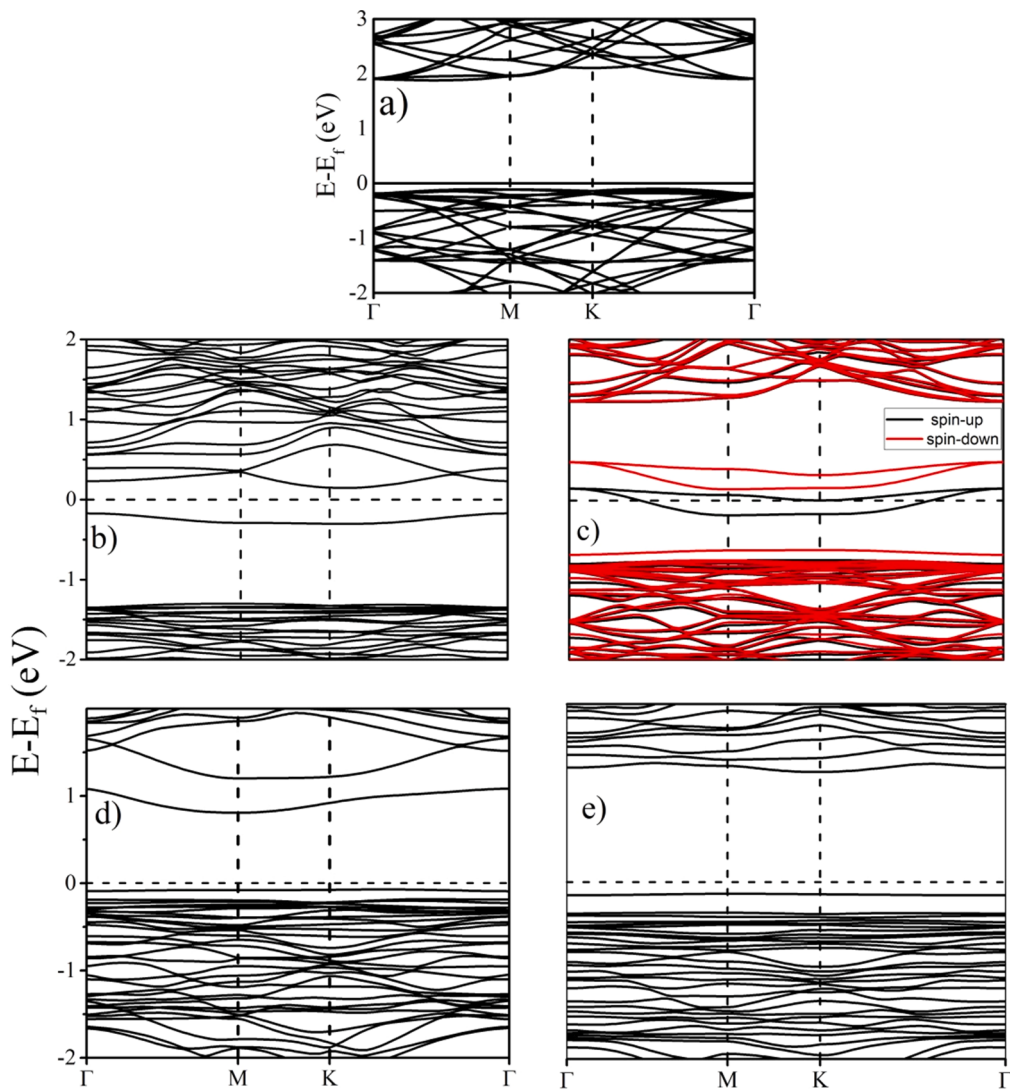


Fig. 5. The band structure plots of a) pristine blue-P; b) SW; c) SV-(5|9); d) DV-(5|8|5); and e) DV-(555|777) defects in blue-P. The black line (red line) in c) represents majority (minority), i.e. up (down) spin carriers.

ev). The calculated adsorption energies, height above different defects, magnetic moment and bond length of hydrogen molecule after adsorption, are shown in the Table 3.

From the adsorption energy values in Table 3, it is seen that SW defect strongly binds, while DV-(555|777) defect binds very weakly, the hydrogen molecule. The adsorption energies in both cases lie outside the optimum range (0.1 eV-1.0 eV) required for a practical hydrogen storage material. In case of SV-(5|9) defect, it is found that the molecule dissociates into two hydrogen atoms and both of them get chemically bonded to the defect with a binding energy -2.88 eV (Fig. 6(b)). This leaves DV-(5|8|5) on which the adsorption energy of hydrogen molecule is optimum. Considering further adsorption of more H₂ molecules over this defect, it is seen that the second hydrogen molecule dissociates, leading to a distorted blue-P sheet and the dissociation of the first hydrogen molecule also. As a result, we get four hydrogen atoms chemically bonded on a distorted blue-P structure (Fig. 6(e)). The adsorption height is highest for DV-(555|777) indicating least binding, and least for SW. In case of SV-(5|9) defect, the spin polarization is retained even after the H₂ molecule is adsorbed on it. The H-H bond length (R in Table 3) has negligible change, from the gas phase value, 0.751 Å. From the DOS calculated for the adsorbed system in Fig. 7, we can see a clear mixing of molecular and blue-P states in all cases, except where hydrogen molecule is very weakly bound in the case of DV-(555|

777) defect. Thus we see that as it is, defective blue-P is unsuitable as a H₂ storage material, even though it has reasonable binding for a single H₂ at DV-(5|8|5).

3.4. Adsorption of lithium atom on defects

The suitability of metal decorated structures for H₂ storage has been investigated in context of graphene and phosphorene earlier [30,36,45]. We have earlier seen [37] that metal decoration of blue-P leads to stronger binding and storage of more H₂ molecules. Extending this now to defective blue-P, we first study how a typical light metal like Li binds to blue-P. Li atoms are adsorbed on to the most favored adsorption site, i. e. hollow site of all the defects. While the adsorption energy of Li atom on defect free blue-P is around 2 eV, here irrespective of the kind of defect, the Li atom is bound more strongly, as seen from Table 4.

In case of SV-(5|9), the magnetic moment of system gets enhanced due the adsorption of Li atom with a magnetic moment $1\mu_B$. In our previous work on Li adsorption on pristine blue-P, we have shown that there is a transfer of 1 electron from Li to blue-P. In case of Li adsorbed over a blue-P with a SV-(5|9) defect, from the analysis of Bader charges, we see that a net charge of 0.9 electrons is transferred to blue-P by Li (see supplementary information). From Fig. 4(c), the DOS at the Fermi level is polarized to one kind of spin for the SV-(5|9) defect. Hence, charge

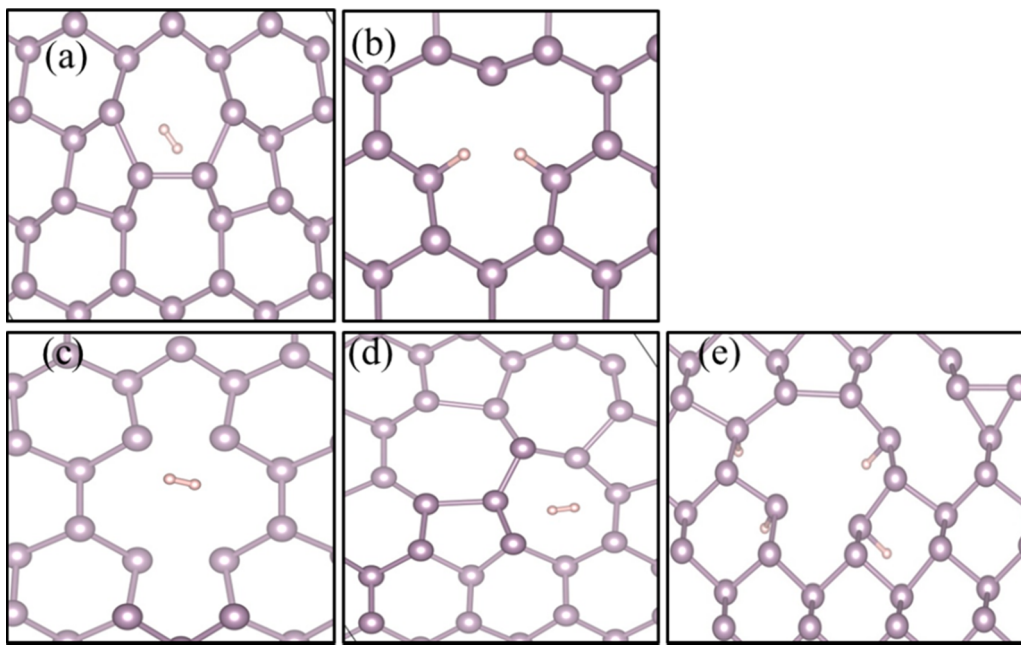


Fig. 6. One hydrogen molecule adsorbed on (a) SW, (b) SV-(5|9), (c) DV-(5|8|5) and (d) DV-(555|777) defects and (e) two hydrogen molecules dissociated on DV-(5|8|5) defect, on a blue-P sheet.

Table 3

The calculated adsorption energy (E_{ads}), the adsorption height (h), the magnetic moment (μ) and H-H bond length (R) of hydrogen molecule adsorbed on various defects in blue-P.

	SW	SV-(5 9)	DV-(5 8 5)	DV-(555 777)
E_{ads} (eV)	1.60	5.76	0.10	0.05
h (Å)	1.47	—	1.53	2.55
μ (μ_B)	0	0.95	0	0
R (Å)	0.753	—	0.753	0.750

transfer from Li will lead to occupancy of the same kind of states, since the states of opposite spin polarization are not available at E_f . This will lead to the enhancement of the magnetic moment of the blue-P, due to Li

Table 4

The adsorption energy (E_{ads}), the magnetic moment (μ) and the height from the lowest P atom to the adsorbed Li when Li as adsorbed on various defects.

	SW	SV-(5 9)	DV-(5 8 5)	DV-(555 777)
E_{ads} (eV)	4.27	3.30	3.28	2.34
Z (Å)	0.0	1.46	0.0	0.0
μ (μ_B)	0.0	2.0	0.0	0.0

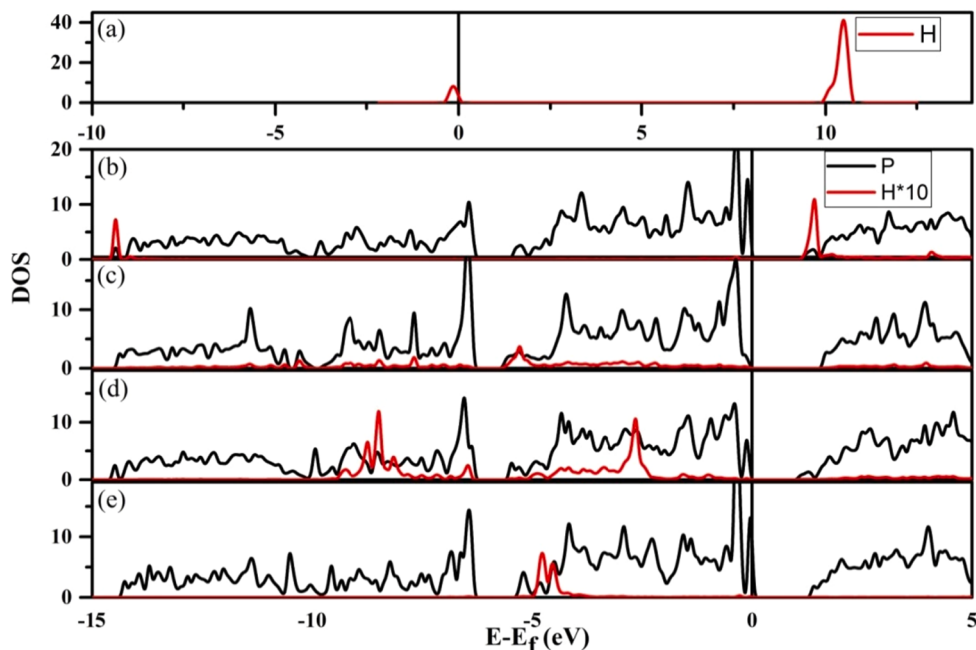


Fig. 7. PDOS of P and H in (a) H_2 molecule; H_2 molecule adsorbed on (b) SW (c) SV-(5|9) (d) DV-(5|8|5) and (e) DV-(555|777) defects on a blue-P sheet.

adsorption. Adsorption of Li on SV-(5|9) defective blue-P is like doping blue-P with an n-type impurity; as seen from the electronic structure (See [supplementary information](#)). Except for SV-(5|9) in which the adsorbed Li is a little elevated from surface, in all the other defects the adsorbed Li is in the plane of the defective blue-P sheet. The fact that the Li atom is not adsorbed exactly on to the 2D sheet leads to the possibility that it can be adsorbed on the both sides of the blue-P sheet, i.e. top and bottom of the SV-(5|9) defect. The adsorbed Li atom on all defects is shown in [Fig. 8](#).

The Li and P projected DOS in [Fig. 9](#) shows shifting of adsorbate states to lower energy and mixing of states which are all clear signs of strong chemisorption of Li on the defects. It is to be noted that the Li-Li cohesive energy [46] turns out to be smaller than the Li-defect binding energies listed in [Table 4](#), hence the possibility that Li would cluster on the blue-P surface is ruled out. Such clustering would be detrimental to increasing H₂ storage, as the molecules would be too close to each other.

3.5. Hydrogen adsorption on defective blue-P decorated with lithium atoms

Since only one H₂ molecule can be effectively adsorbed on defective blue-P sheets, we now seek if Li decoration of the defect sites can increase the number of H₂. In SW and DV-(5|8|5) defects, even though the first H₂ molecule gets adsorbed on the Li atom decorated with defects with energies, 0.33 eV and 0.27 eV respectively (both at a height 1.97 Å from Li atom), a second hydrogen molecule does not get adsorbed on to either of these Li decorated defects i.e., the adsorption energy falls below 0.1 eV. The structures of defects with one molecule each is shown in [Fig. 10\(a\)](#) and [\(c\)](#). In case of SV-(5|9) defect, the Li atom accommodates more than two H₂ molecules. In [Fig. 10 \(b\)](#), the Li decorated relaxed structure of a SV-(5|9) defect carrying five adsorbed H₂ molecules is displayed. In the case of DV-(555|777) defect, it is found that up-to two hydrogen molecules get adsorbed on a Li atom (with adsorption energies 0.32 eV and 0.19 eV respectively) at heights 0.74 Å and 1.72 Å from the Li atom respectively (see [Fig. 10\(d\)](#)).

Coming to the case of Li-decorated SV-(5|9) defect, the five hydrogen molecules get adsorbed at heights ranging from 0.75 Å to 1.2

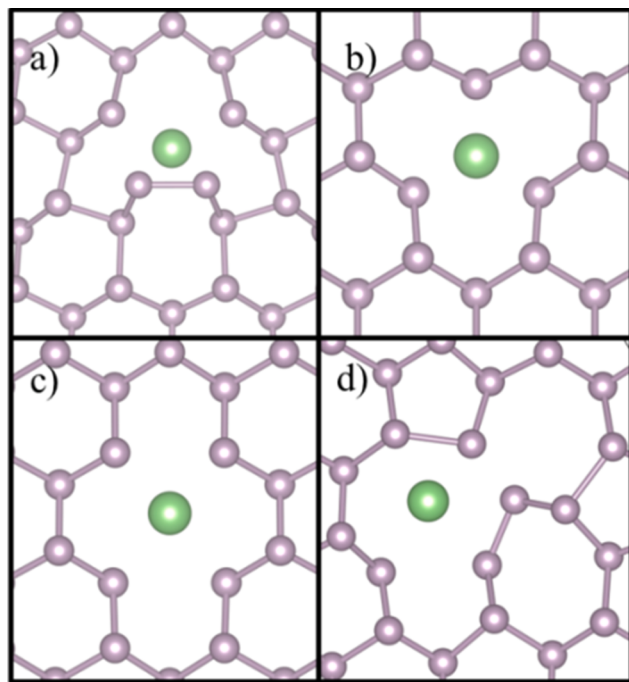


Fig. 8. Optimized geometries of lithium atom adsorbed on all four defects, at the hollow position on blue-P sheet.

Å from the Li atom with adsorption energies ranging from 0.11 eV to 0.26 eV. The DOS of all these configurations are shown in [Fig. 11\(a\)-\(e\)](#). The overlap of the PDOS of Li atom and H₂ molecules establish the interaction between these atoms. All of these systems remain magnetic with a magnetic moment 2.0 μB. New peaks are found in the DOS when H₂ molecules are added on the substrate one by one and we can see clear mixing of these states with the states of lithium atom, proving that there is some kind of bonding taking place between these. The details of calculated adsorption energies of H₂ molecules over various defect sites decorated by Li is in the [supplementary material](#).

For further analysis of the interaction between H₂ molecules and SV-(5|9) defective blue-P, the difference charge density (DCD) for the system in the ground state is calculated. The difference charge density is defined as $\rho_{\text{diff}} = (\rho_X + \rho_{H_2}) - \rho_{\text{total}}$, with ρ_X and ρ_{H_2} being the charge density of the substrate and H₂ molecule in their ground states, and ρ_{total} the charge density of substrate and adsorbate. The DCD for this system is shown in [Fig. 12\(b\)](#). All the hydrogen molecules are polarized by the Li atom which in turn leads to the adsorption binding. The type of intermediate strength H₂ binding we find in these systems cannot be classified as a case of chemisorption, which would result in binding energies of the order of 1 eV or above. From our previous studies [37] with pristine blue-P, we have found that there is a significant charge transfer between Li and P, and the positively charged Li polarizes the H₂ molecule and binds it. A slight elongation of the H-H bond is seen here. For the case of H₂ adsorbed on transition metals, Kubas et al. [49] propose a mechanism which apply for adsorption energies from 100 meV to 1 eV (from weak vdW regime to a strong chemisorption regime). The bonding interaction results in a charge transfer between the substrate and the molecule, in which the molecule transfers some charge to the unoccupied d states of transition metal, while a reverse transfer takes place from metal d states to the antibonding levels of H₂, leading to a slight elongation of the H-H bond. This is suggestive of similar scenario, in which a transfer of electrons occurs to the half-filled ns states of alkali metal and a reverse donation from alkali atom to the anti-bonding levels of H₂ molecule takes place. The details of the energetics and states involved needs to be further investigated.

3.6. Thermal stability of adsorbed configurations

Ab-initio molecular dynamics (MD) calculations at constant volume were performed to study the thermal stability of the adsorbed system. Simulations with a time step of 1.0 fs were carried out in the canonical ensemble at approximately room temperature using the Nose-Hoover thermostat [47,48] for the temperature control. For these calculations, the initial state (att = 0) is taken to be the geometry optimized structure. We find that, like in black-P [20], point defects are stable at room temperatures in blue-P also. We have studied the time evolution of hydrogen molecules adsorbed over Li decorated SV-(5|9) defect and find that the configuration is dynamically stable at room temperature (see [supplementary information](#)). The adsorption height of H₂ over lithium at 300 K changes on an average by 11% from the value at 0 K. Thus, we predict that these materials can act as potential candidates for hydrogen storage at room temperature. These calculations have been performed for the SV-(5|9) defect only, to reduce the number of expensive MD simulations.

3.7. Hydrogen adsorption on defects decorated with multiple lithium atoms

We have investigated how increasing the Li atom coverage over the defect changes the number of H₂ adsorbed. The fact that Li atom gets elevated above the sheet when adsorbed on top of SV-(5|9) defect gives room for two Li to be adsorbed on both sides of the SV-(5|9) defect. We have also attempted to add more Li to the SV-(5|9) defect; addition of two Li on the same side within the defect gives stable binding of Li to

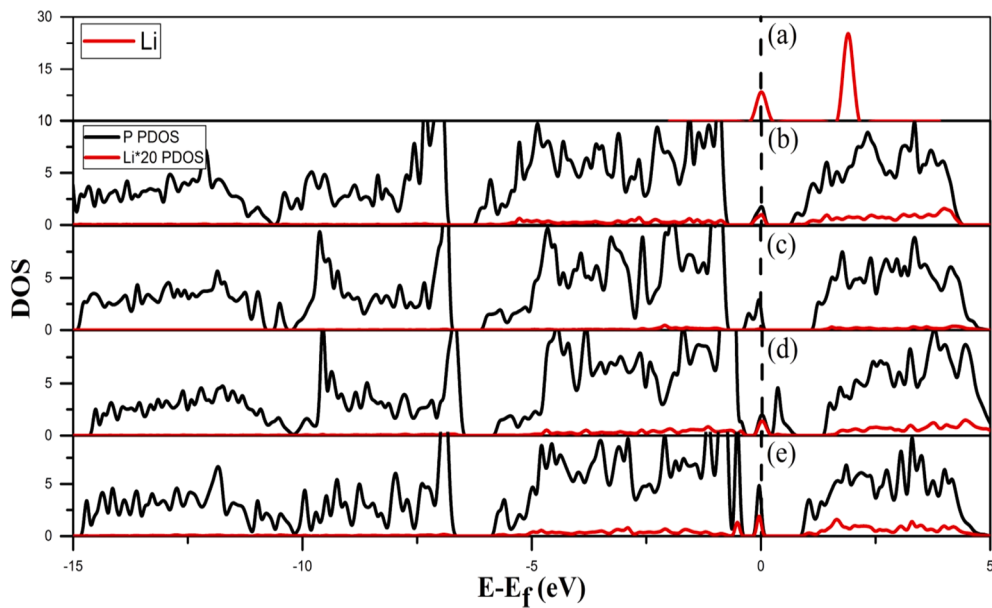


Fig. 9. Projected DOS of P and Li in (a) Li atom; Li adsorbed on (b) SW defect; (c) SV-(5|9) defect; (d) DV-(5|8|5) defect and (e) DV-(555|777) defect, showing mixing of adsorbate and surface states and shift of adsorbate states to lower energy.

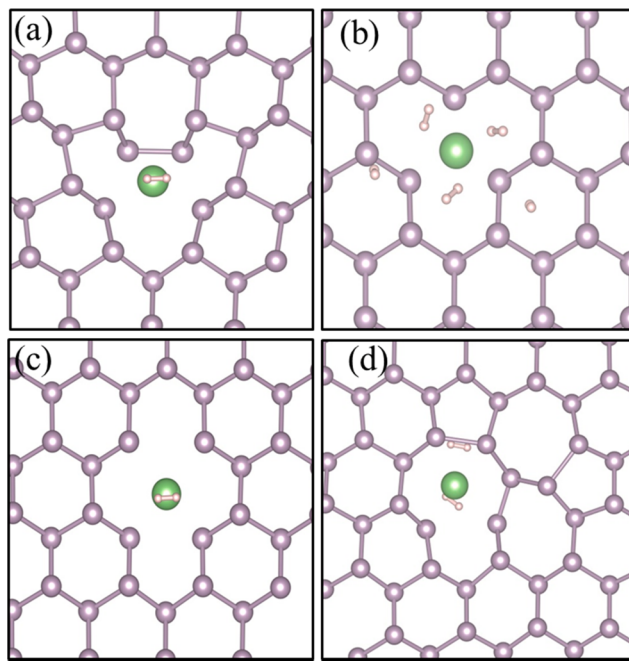


Fig. 10. The structures of Li decorated (a) SW and (c) DV-(5|8|5) defects with one molecule of hydrogen adsorbed on them; (b) SV-(5|9) defect with five molecules of hydrogen adsorbed; (d) DV-(555|777) defect with two molecules of hydrogen adsorbed on it.

blue-P. However, if we try to add a third Li, one of the Li atoms moves over to the other side of the sheet. Adsorption of H₂ for these Li atoms would give stable configurations of three H₂ (one per Li). Further addition of H₂ does not lead to six H₂ in a stable configuration (two per Li); one of the H₂ dissociates. Hence, we conclude that the SV-(5|9) defect may not store more than five H₂ molecules in a stable configuration. Further Li decorations are therefore not productive. It is also noted that there are three symmetrically equivalent adsorption sites on the defect DV-(555|777), hence up to three Li atoms can possibly adsorb on to a DV-(555|777) defect. Within the context of these configurations,

calculations show that up to six molecules (three on each Li atom) can be adsorbed on SV-(5|9) (Fig. 13(a) and (b)) and up to nine hydrogen molecules (three on each Li atom) can be adsorbed on DV-(555|777) ((Fig. 13(c) and (d)). The gravimetric storage capacity (%) C may be defined as $C = \frac{w}{W} \times 100$, where w is weight of adsorbed H₂ molecules, and W the weight of adsorbent and substrate together (for details, see [supplementary information](#)). In case of an SV-(5|9) defect in blue-P decorated with two Li atoms, when 6 H₂ molecules are adsorbed, we get a gravimetric storage capacity of 6.02% when all other phosphorus atoms are considered to be non-defective. This being the contribution from a single type of defect, we can clearly say that the presence of these defects and their decoration with Li or similar metals will definitely enhance the hydrogen storage capabilities of blue-P.

In case of the DV-(555|777) defect, we would expect that C is much higher, for there are 3 H₂ molecules adsorbed on to 3Li atoms each. Calculations give a C value only marginally higher, i.e. 6.42%. From the geometry of the adsorbed structures as seen from Fig. 13 (d) for the DV-(555|777) defect, we can expect that more Li atoms are accommodated per defect, since the equilibrium structure has Li atoms resting not in the blue-P sheet; hence both sides of the sheet may be used to adsorb these, as seen in case of SV-(5|9). However, we find that the number of H₂ molecules adsorbed will then reduce, resulting in almost no change in the gravimetric capacity. Thus, we may conclude that both SV-(5|9) defect and DV-(555|777) defect can yield a gravimetric ratio of above 6%. The presence of a large number of these defects decorated by Li atoms can then lead to improved storage of H₂.

3.8. Comparing blue and black-P

Black-P is the better known and studied amongst the phosphorene allotropes. Its capacity to adsorb and store H₂ molecules has been explored in considerable detail by Halder et al. [38]. It is found that defective black-P by itself does not give any useful storage of H₂, like the case of blue-P. Also, the binding energy of H₂ is too low on defects, in the range of 0.03–0.06 eV. They find that Li decoration of SV-(5|9) defect leads to stronger adsorption of H₂, with adsorption energy in the range 0.48 eV. We have also repeated calculations on black-P for completeness of our studies. We find that SV-(5|9) defect in black-P, upon Li decoration, can adsorb two molecules of H₂ effectively, as shown in Fig. 14, without dissociation. Halder et al. estimate a gravimetric storage

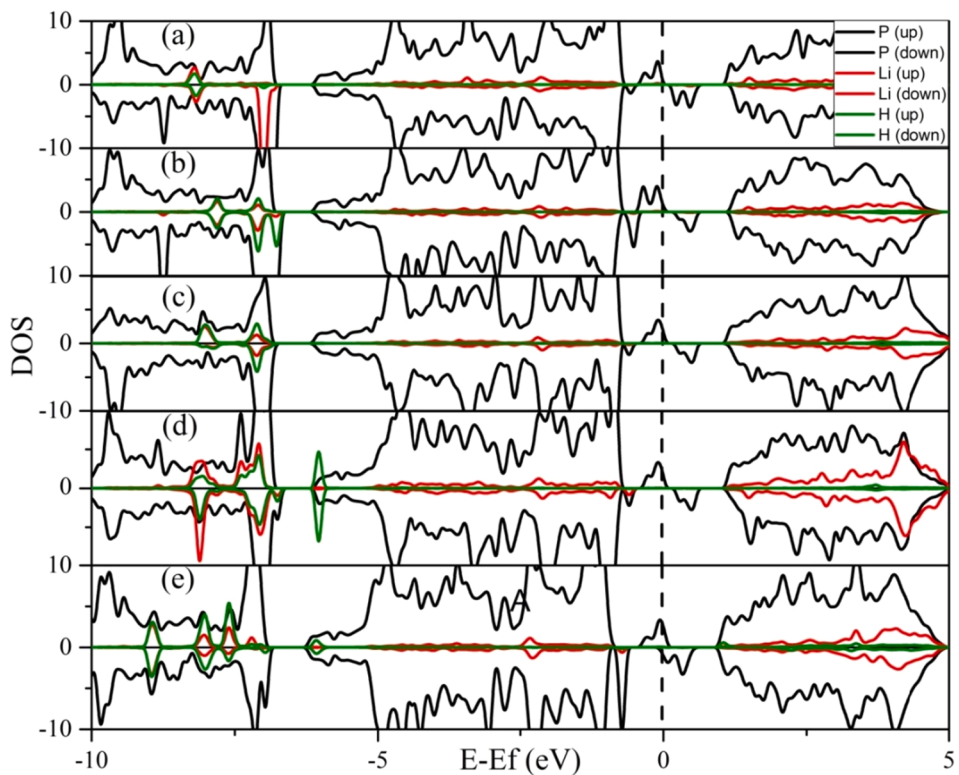


Fig. 11. The DOS plots of (a) one (b) two (c) three (d) four and (e) five hydrogen molecules adsorbed on Li decorated SV-(5|9) defect.

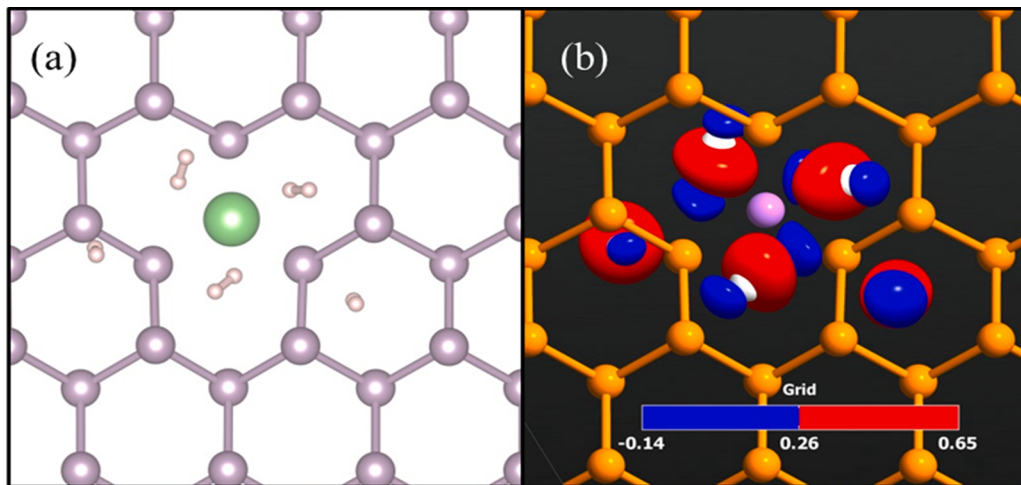


Fig. 12. (a) The relaxed structure of five hydrogen molecules adsorbed on Li decorated SV-(5|9) defect and (b) the difference charge density plot (DCD) of the same, plotted using an iso-surface value 0.05 electrons/Å³.

capacity of 5.3% on defective black-P, while defective blue-P has an enhanced 6.42% storage. It can be concluded that for real materials, with a combination of non-defective lattice and point defects, decorated with light metals like Li, blue-P is able to store a greater number of H₂ than black-P.

3.9. Comparing with other nanomaterials

Recent research has discovered that metal oxide and hydride clusters and nanosheets have been found to be very suitable for storage of H₂, like in (Al₂O₃)_n (n = 2–5) [50], (BeO)_n (n = 2–8) [51], (MgO)₁₂ nano clusters [52], hydrogen boride nanosheets (HB sheets) [53] and manganese hydride molecular sieve [54]. As mentioned in the introduction,

these materials are a motivation to explore the possibilities of H₂ storage in other nanomaterials, especially 2D nanosheets. These materials exhibit higher storage capabilities, ranging from 7% to 11% gravimetric storage capacity, whereas blue-P / black-P or defective blue-P / black-P do not measure up to the same capacity of storage. Nanosheets of the 2D material C₂N decorated with Li have an exceptionally high theoretical gravimetric capacity of 13% [55]. Studies of metal decoration of 2D materials and exploration of defect nanostructures are important to predict better hydrogen storage materials in future.

4. Summary and conclusions

Point defects in 2D blue-P nano sheet like Stone-Wales (SW), single

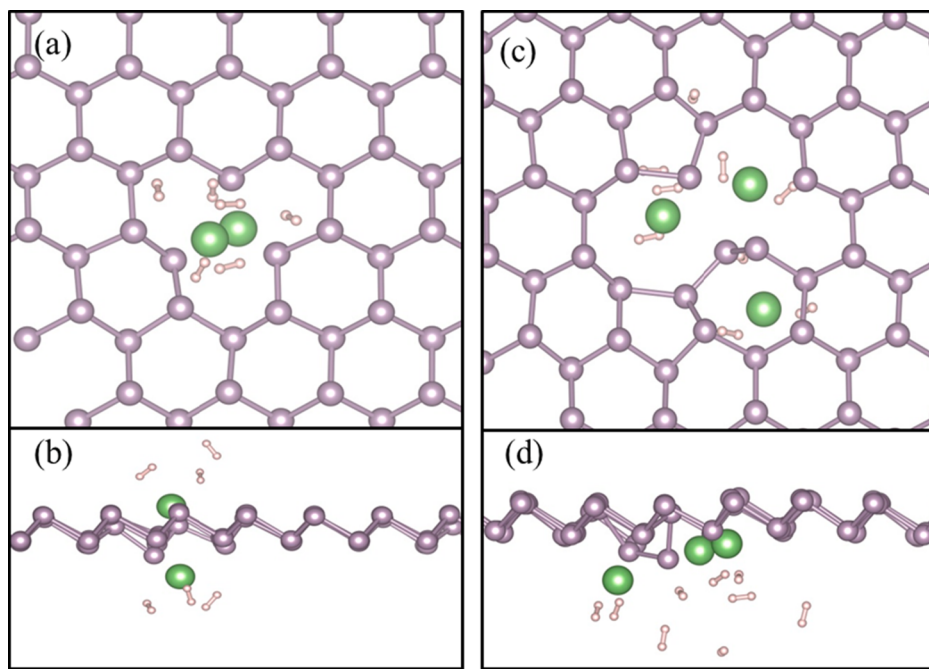


Fig. 13. Six hydrogen molecules adsorbed on SV-(5|9) defect decorated with two Li atoms (a) top view and (b) side view. Nine hydrogen molecules adsorbed on DV-(555|777) defect decorated with three Li atoms (c) top view and (d) side view.

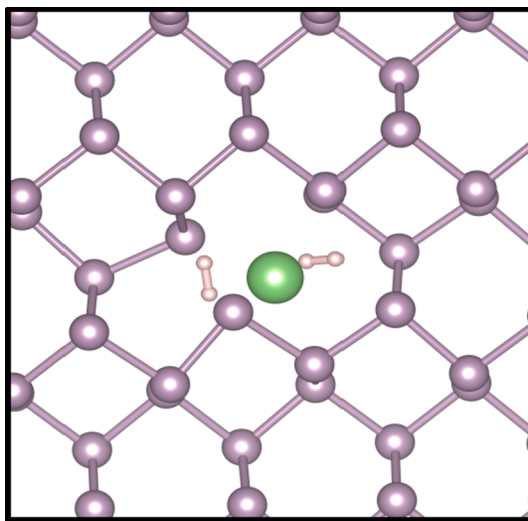


Fig. 14. The relaxed structure of two hydrogen molecules adsorbed on Li decorated SV-(5|9) defect in black-P.

vacancy (SV-(5|9)) and double vacancy defects (DV-(5|8|5), DV-(555|777)) were systematically simulated and studied. H₂ molecule is found to be weakly bound to the defects, to be of any practical importance to largescale storage. Li atoms are chemisorbed on to these defects in order to bind H₂ better. Adsorption energy of H₂ molecules on Li-decorated defects is found to be within the required range to be practically useful. Up-to five hydrogen molecules could be adsorbed on SV-(5|9) defect. On increasing the coverage of lithium atoms, up-to six molecules (three on each Li atom) can be adsorbed on two Li decorated SV-(5|9) defects and up-to nine H₂ (three on each Li atom) can be adsorbed on three Li decorated DV-(555|777). Ab-initio MD simulations show metal decorated defective blue-P structures holding adsorbed H₂ to be stable at 300 K. Comparing with Li decorated defective blue-P and defective black-P, the SV-(5|9) in the former can hold up to five while in the latter it can hold only up to two H₂ molecules. To summarize, the gravimetric

storage density of H₂ molecules is predicted to be greater in Li decorated defective blue-P than in Li decorated pristine blue-P and Li decorated defective black-P. These results are likely to hold for decoration with other light metals like Na or Mg, as was found in case of pristine blue-P. Thus blue-P, with random defects which occur naturally in these as a result of manufacturing processes, would be a better storage template for H₂, when decorated by light metals.

CRediT authorship contribution statement

Daughty John: Conceptualization. **Bijoy Nharangatt:** ab-initio MD Computation. **Srihari Madhav Kastaur:** Validation. **Raghu Chatanathodi:** Conceptualization.

Declaration of Competing Interest

The authors declare that they have no known competing financial interests or personal relationships that could have appeared to influence the work reported in this paper.

Appendix A. Supplementary material

Supplementary data to this article can be found online at <https://doi.org/10.1016/j.apsusc.2021.149363>.

References

- [1] A.H. Castro Neto, F. Guinea, N.M.R. Peres, K.S. Novoselov, A.K. Geim, The electronic properties of graphene, Rev. Mod. Phys. 81 (2009) 109–162, <https://doi.org/10.1103/RevModPhys.81.109>.
- [2] S.Z. Butler, S.M. Hollen, L. Cao, Y. Cui, J.A. Gupta, H.R. Gutierrez, T.F. Heinz, S. Hong, J. Huang, A.F. Ismach, E. Johnston-Halperin, M. Kuno, V.V. Plashnitsa, R. D. Robinson, R.S. Ruoff, S. Salahuddin, J. Shan, L. Shi, M.G. Spencer, M. Terrones, W. Windl, J.E. Goldberger, Progress, challenges, and opportunities in two-dimensional materials beyond graphene, ACS Nano 7 (2013) 2898–2926, <https://doi.org/10.1021/nm400280c>.
- [3] G.G. Guzmán-Verri, L.C. Lew Yan Voon, Electronic structure of silicon-based nanostructures, Phys. Rev. B - Condens. Matter Mater. Phys. (2007). <https://doi.org/10.1103/PhysRevB.76.075131>.
- [4] A.K. Geim, K.S. Novoselov, The rise of graphene, in: Nanosci. Technol. A Collect. Rev. from Nat. Journals, 2009. https://doi.org/10.1142/9789814287005_0002.

- [5] S. Cahangirov, M. Topsakal, E. Aktürk, H. Şahin, S. Ciraci, Two- and one-dimensional honeycomb structures of silicon and germanium, *Phys. Rev. Lett.* (2009), <https://doi.org/10.1103/PhysRevLett.102.236804>.
- [6] Y. Jing, X. Zhang, Z. Zhou, Phosphorene: What can we know from computations? *Wiley Interdiscip. Rev. Comput. Mol. Sci.* (2016) <https://doi.org/10.1002/wcms.1234>.
- [7] H. Liu, A.T. Neal, Z. Zhu, Z. Luo, X. Xu, D. Tománek, P.D. Ye, Phosphorene: an unexplored 2D semiconductor with a high hole mobility, *ACS Nano* 8 (2014) 4033–4041, <https://doi.org/10.1021/nm501226z>.
- [8] Z. Zhang, E.S. Penev, B.I. Yakobson, Two-dimensional boron: structures, properties and applications, *Chem. Soc. Rev.* 46 (2017) 6746–6763, <https://doi.org/10.1039/c7cs00261k>.
- [9] B. Feng, J. Zhang, Q. Zhong, W. Li, S. Li, H. Li, P. Cheng, S. Meng, L. Chen, K. Wu, Experimental realization of two-dimensional boron sheets, *Nat. Chem.* (2016), <https://doi.org/10.1038/nchem.2491>.
- [10] M. Li, Y. Li, Z. Zhou, P. Shen, Z. Chen, Ca-Coated boron fullerenes and nanotubes as superior hydrogen storage materials, *Nano Lett.* (2009), <https://doi.org/10.1021/nl900116q>.
- [11] H. Wang, C. Li, P. Fang, Z. Zhang, J.Z. Zhang, Synthesis, properties, and optoelectronic applications of two-dimensional MoS₂ and MoS₂-based heterostructures, *Chem. Soc. Rev.* 47 (2018) 6101–6127, <https://doi.org/10.1039/c8cs00314a>.
- [12] Z. Zhu, D. Tománek, Semiconducting layered blue phosphorus: a computational study, *Phys. Rev. Lett.* 112 (2014), <https://doi.org/10.1103/PhysRevLett.112.176802>.
- [13] J.L. Zhang, S. Zhao, C. Han, Z. Wang, S. Zhong, S. Sun, R. Guo, X. Zhou, C.D. Gu, K. Di Yuan, Z. Li, W. Chen, Epitaxial growth of single layer blue phosphorus: a new phase of two-dimensional phosphorus, *Nano Lett.* 16 (2016) 4903–4908, <https://doi.org/10.1021/acs.nanolett.6b01459>.
- [14] V. Sorkin, Y. Cai, Z. Ong, G. Zhang, Y.W. Zhang, Recent advances in the study of phosphorene and its nanostructures, *Crit. Rev. Solid State Mater. Sci.* 42 (2017) 1–82, <https://doi.org/10.1080/10408436.2016.1182469>.
- [15] L. Qiu, J.C. Dong, F. Ding, Selective growth of two-dimensional phosphorene on catalyst surface, *Nanoscale*. 10 (2018) 2255–2259, <https://doi.org/10.1039/c7nr08507a>.
- [16] F. Banhart, J. Kotakoski, A.V. Krasheninnikov, Structural defects in graphene, *ACS Nano* 5 (2011) 26–41, <https://doi.org/10.1021/nn102598m>.
- [17] L. Weston, D. Wickramaratne, M. Mackoit, A. Alkauskas, C.G. Van De Walle, Native point defects and impurities in hexagonal boron nitride, *Phys. Rev. B.* (2018), <https://doi.org/10.1103/PhysRevB.97.214104>.
- [18] G. Do Lee, C.Z. Wang, E. Yoon, N.M. Hwang, D.Y. Kim, K.M. Ho, Diffusion, coalescence, and reconstruction of vacancy defects in graphene layers, *Phys. Rev. Lett.* 95 (2005), <https://doi.org/10.1103/PhysRevLett.95.205501>.
- [19] J. Gao, J. Zhang, H. Liu, Q. Zhang, J. Zhao, Structures, mobilities, electronic and magnetic properties of point defects in silicene, *Nanoscale*. 5 (2013) 9785–9792, <https://doi.org/10.1039/c3nr02826g>.
- [20] W. Hu, J. Yang, Defects in phosphorene, *J. Phys. Chem. C.* 119 (2015) 20474–20480, <https://doi.org/10.1021/acs.jpcc.5b06077>.
- [21] B. Sa, Y.L. Li, J. Qi, R. Ahuja, Z. Sun, Strain engineering for phosphorene: the potential application as a photocatalyst, *J. Phys. Chem. C.* 118 (2014) 26560–26568, <https://doi.org/10.1021/jp508618t>.
- [22] W. Li, Y. Yang, G. Zhang, Y.W. Zhang, Ultrafast and directional diffusion of lithium in phosphorene for high-performance lithium-ion battery, *Nano Lett.* 15 (2015) 1691–1697, <https://doi.org/10.1021/nl504336h>.
- [23] V.V. Kulish, O.I. Malyi, C. Persson, P. Wu, Phosphorene as an anode material for Na-ion batteries: a first-principles study, *Phys. Chem. Chem. Phys.* 17 (2015) 13921–13928, <https://doi.org/10.1039/c5cp01502b>.
- [24] J.M. Ogden, Prospects for building a hydrogen energy infrastructure, *Annu. Rev. Energy Environ.* (1999), <https://doi.org/10.1146/annurev.energy.24.1.227>.
- [25] S.A. Shevlin, Z.X. Guo, Density functional theory simulations of complex hydride and carbon based hydrogen storage materials, *Chem. Soc. Rev.* 38 (2009) 211–225, <https://doi.org/10.1039/b81553b>.
- [26] S.K. Bhatia, A.L. Myers, Optimum conditions for adsorptive storage, *Langmuir* 22 (2006) 1688–1700.
- [27] N. Park, K. Choi, J. Hwang, D.W. Kim, D.O. Kim, J. Ihm, Progress on first-principles-based materials design for hydrogen storage, *Proc. Natl. Acad. Sci.* 109 (2012) 19893–19899.
- [28] W. Liu, Y.H. Zhao, Y. Li, Q. Jiang, E.J. Lavernia, Enhanced hydrogen storage on li-disperse carbon nanotubes, *J. Phys. Chem. C.* 113 (2009) 2028–2033, <https://doi.org/10.1021/jp8091418>.
- [29] H. Yelu, W. Shuxia, Hydrogen storage of platinum atoms adsorbed on graphene: First-principles plane wave calculations, *Appl. Mech. Mater.* 246–247 (2013) 1057–1060, <https://doi.org/10.4028/www.scientific.net/AMM.246-247.1057>.
- [30] E. Durgun, S. Ciraci, T. Yildirim, Functionalization of carbon-based nanostructures with light transition-metal atoms for hydrogen storage, *Phys. Rev. B - Condens. Matter Mater. Phys.* 77 (2008), <https://doi.org/10.1103/PhysRevB.77.085405>.
- [31] E. Durgun, S. Ciraci, W. Zhou, T. Yildirim, Transition-metal-ethylene complexes as high-capacity hydrogen-storage media, *Phys. Rev. Lett.* 97 (2006), <https://doi.org/10.1103/PhysRevLett.97.226102>.
- [32] Q. Sun, P. Jena, Q. Wang, M. Marquez, First-principles study of hydrogen storage on Li₁₂C₆₀, *J. Am. Chem. Soc.* 128 (2006) 9741–9745, <https://doi.org/10.1021/ja058330c>.
- [33] W.Q. Deng, X. Xu, W.A. Goddard, New alkali doped pillared carbon materials designed to achieve practical reversible hydrogen storage for transportation, *Phys. Rev. Lett.* 92 (2004), <https://doi.org/10.1103/PhysRevLett.92.166103>.
- [34] E. Klontzas, A. Mavrandonakis, E. Tylianakis, G.E. Froudakis, Improving hydrogen storage capacity of MOF by functionalization of the organic linker with lithium atoms, *Nano Lett.* 8 (2008) 1572–1576, <https://doi.org/10.1021/nl072941g>.
- [35] M. Yoon, S. Yang, C. Hicke, E. Wang, D. Geohegan, Z. Zhang, Calcium as the superior coating metal in functionalization of carbon fullerenes for high-capacity hydrogen storage, *Phys. Rev. Lett.* 100 (2008), <https://doi.org/10.1103/PhysRevLett.100.206806>.
- [36] Z. Yu, N. Wan, S. Lei, H. Yu, Enhanced hydrogen storage by using lithium decoration on phosphorene, *J. Appl. Phys.* 120 (2016), <https://doi.org/10.1063/1.4958695>.
- [37] D. John, R. Chatanathodi, Hydrogen adsorption on alkali metal decorated blue phosphorene nanosheets, *Appl. Surf. Sci.* 465 (2019) 440–449, <https://doi.org/10.1016/j.apsusc.2018.09.158>.
- [38] S. Haldar, S. Mukherjee, F. Ahmed, C.V. Singh, A first principles study of hydrogen storage in lithium decorated defective phosphorene, *Int. J. Hydrogen Energy.* 42 (2017) 23018–23027, <https://doi.org/10.1016/j.ijhydene.2017.07.143>.
- [39] G. Kresse, J. Furthmüller, Efficient iterative schemes for ab initio total-energy calculations using a plane-wave basis set, *Phys. Rev. B - Condens. Matter Mater. Phys.* 54 (1996) 11169–11186, <https://doi.org/10.1103/PhysRevB.54.11169>.
- [40] G. Kresse, J. Hafner, Imitation method, *Phys. Rev. B.* 47 (1992) 558–561, <https://doi.org/10.1103/PhysRevB.47.558>.
- [41] J.P. Perdew, K. Burke, M. Ernzerhof, Generalized gradient approximation made simple, *Phys. Rev. Lett.* 77 (1996) 3865–3868, <https://doi.org/10.1103/PhysRevLett.77.3865>.
- [42] S. Grimme, Semiempirical GGA-type density functional constructed with a long-range dispersion correction, *J. Comput. Chem.* 27 (2006) 1787–1799, <https://doi.org/10.1002/jcc.20495>.
- [43] I. Hamada, Van der Waals density functional made accurate, *Phys. Rev. B - Condens. Matter Mater. Phys.* 89 (2014), <https://doi.org/10.1103/PhysRevB.89.121103>.
- [44] H.J. Monkhorst, J.D. Pack, Special points for Brillouin-zone integrations, *Phys. Rev. B.* 13 (1976) 5188–5192, <https://doi.org/10.1103/PhysRevB.13.5188>.
- [45] C. Ataca, E. Aktürk, S. Ciraci, Hydrogen storage of calcium atoms adsorbed on graphene: First-principles plane wave calculations, *Phys. Rev. B.* (2009), <https://doi.org/10.1103>.
- [46] R.A. Silverman, W. Kohn, On the cohesive energy of metallic lithium [20], *Phys. Rev.* 80 (1950) 912–913, <https://doi.org/10.1103/PhysRev.80.912>.
- [47] W.G. Hoover, Canonical dynamics: Equilibrium phase-space distributions, *Phys. Rev. A.* (1985), <https://doi.org/10.1103/PhysRevA.31.1695>.
- [48] S. Nosé, A unified formulation of the constant temperature molecular dynamics methods, *J. Chem. Phys.* (1984), <https://doi.org/10.1063/1.447334>.
- [49] G. Kubas, Metal-dihydrogen and σ-bond coordination: the consummate extension of the Dewar-Chatt-Duncanson model for metal-olefin π bonding, *J. Organomet. Chem.* 635 (2001) 37–68.
- [50] Jiao Sun, Lu, Wen-Cai, Wei Zhang, Li-Zhen Zhao, Ze-Sheng Li, Chia-Chung Sun, Theoretical Study on (Al₂O₃)_n (n = 1–10 and 30) Fullerenes and H₂ Adsorption Properties, *Inorg. Chem.* 47 (7) (2008) 2274–2279, <https://doi.org/10.1021/ic7011364>.
- [51] Shinde, Ravindra, and MeenakshiTayade. Remarkable hydrogen storage on beryllium oxide clusters: first-principles calculations. *The Journal of Physical Chemistry C* 118,31, (2014), 17200–17204, <https://doi.org/10.1021/jp4109943>.
- [52] Dan Luo, et al., Electronic structure and hydrogen storage properties of Li-decorated single layer blue phosphorus, *Int. J. Hydrogen Energy* 43 (17) (2018) 8415–8425, <https://doi.org/10.1016/j.ijhydene.2018.03.115>.
- [53] Kawamura, Reiya, et al. Photoinduced hydrogen release from hydrogen boride sheets. *Nature communications* 10,1, (2019), 1–8, <https://doi.org/10.1038/s41467-019-12903-1>.
- [54] Morris, Leah, et al. A manganese hydride molecular sieve for practical hydrogen storage under ambient conditions. *Energy & Environmental Science* 12,5, (2019), 1580–1591, <https://doi.org/10.1039/C8EE02499E>.
- [55] Arqum Hashmi, et al., Ultra-high capacity hydrogen storage in a Li decorated two-dimensional C 2 N layer, *J. Mater. Chem. A* 5 (6) (2017) 2821–2828, <https://doi.org/10.1039/C6TA08924K>.